

# Deuteron Formation for Big Bang Nucleosynthesis Models

Katrina Koehler <sup>1</sup>, Jennifer French <sup>2</sup>, Brian Daub <sup>2</sup>, Vlad Henzl <sup>2</sup>, June Matthews <sup>2</sup>, Steve Wender <sup>3</sup>, and Mark Yuly <sup>1</sup>

<sup>1</sup> Houghton College, One Willard Avenue, Houghton NY 14744

<sup>2</sup> Massachusetts Institute of Technology, 77 Massachusetts Avenue, Cambridge, MA 02139

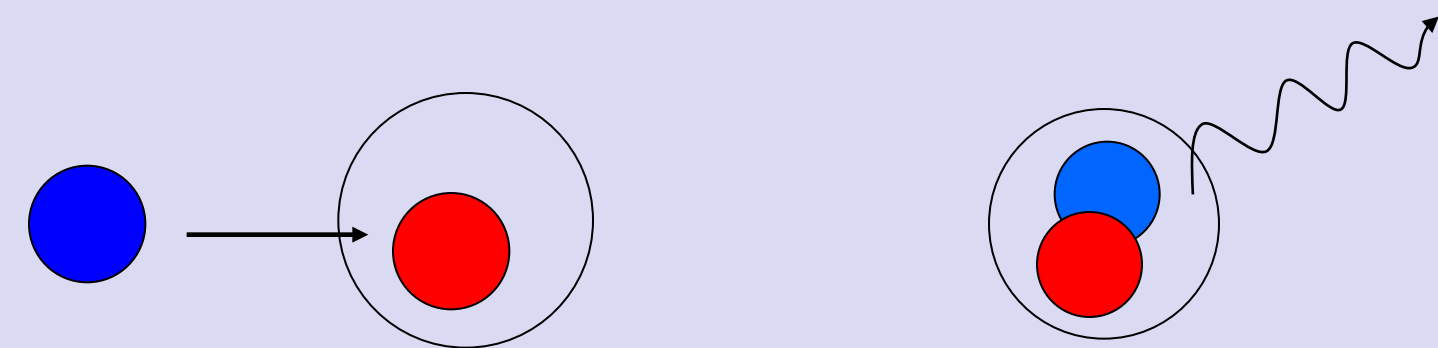
<sup>3</sup> Los Alamos National Lab, Los Alamos, NM 87545

## I. Abstract

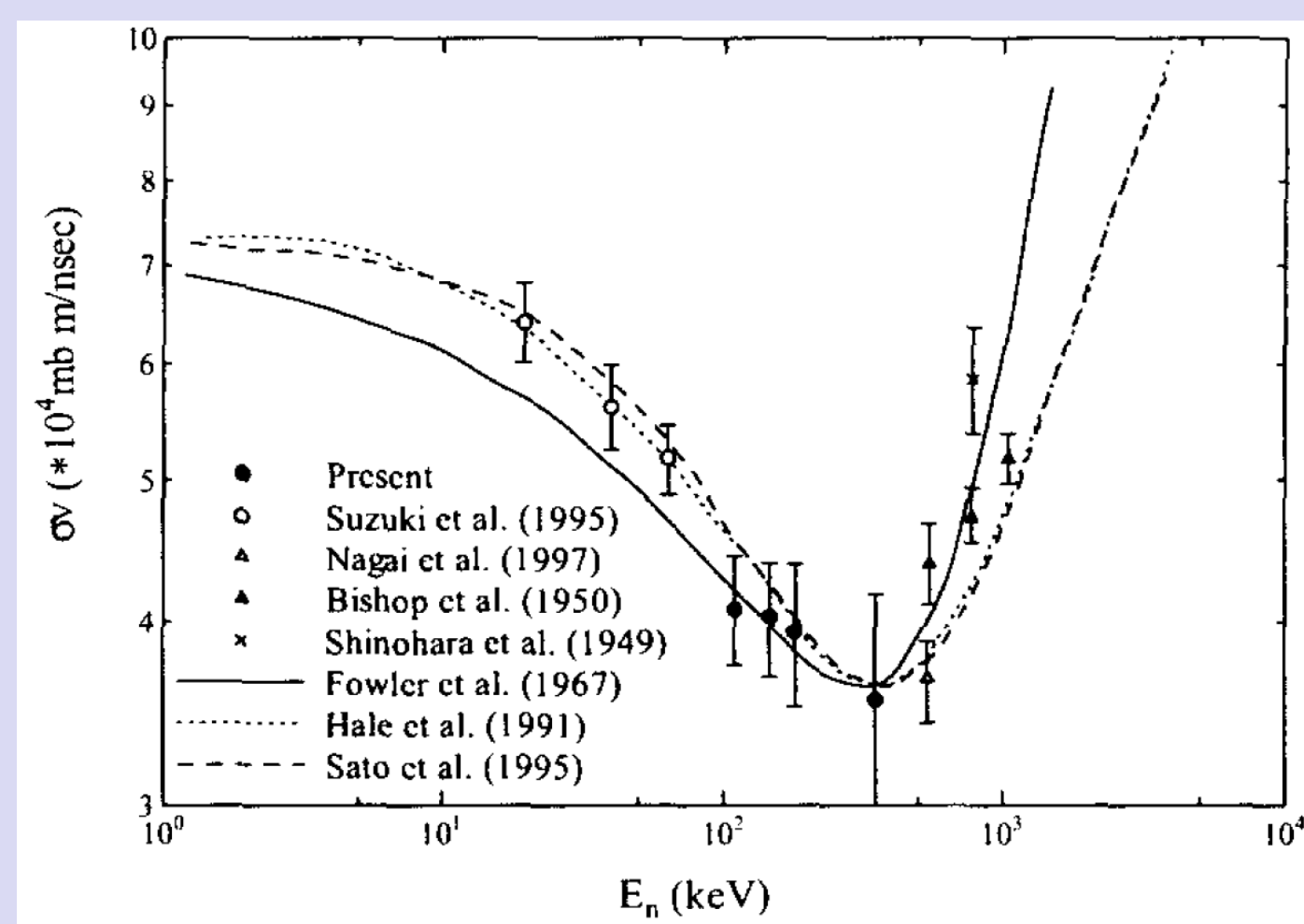
A measurement of the  $H(n, d\gamma)$  cross section at low energy is being performed on flight path 15R from Target 4 at WNR with incident neutron energies between 100 keV and 1 MeV. This deuteron formation experiment is key to improving calculations of the baryon density in Big Bang Nucleosynthesis models. The deuterons are created and detected in a plastic scintillator active target. Gamma rays released by the neutron-proton capture reaction are detected in a BrillLanCe detector. Scattered neutrons from n-p elastic scattering detected in two neutron detectors are used for calibrating the active target ADC spectrum.

## II. Motivation

Big Bang Nucleosynthesis models predict that the relative abundances of light elements, such as H, He and Li, are dependent on the baryon density in the early universe. Different isotopes of these elements have different dependencies, and deuterium is the most sensitive of these isotopes, making it the “baryometer of choice” [1]. Measurements have been made of the present deuterium abundance. By comparing this abundance to the abundances of the other light elements, the baryon density can be calculated. The baryon density of the universe is important in many equations that describe the time evolution and spatial geometry of our universe. Half of the uncertainty in this calculated baryon density is due to uncertainty in the cross section of the  $n + p \rightarrow d + \gamma$  reaction [2].



In neutron capture, the target proton captures the incident neutron, forming a deuteron and releasing a 2.225 MeV gamma ray with an additional half the energy of the incident neutron.

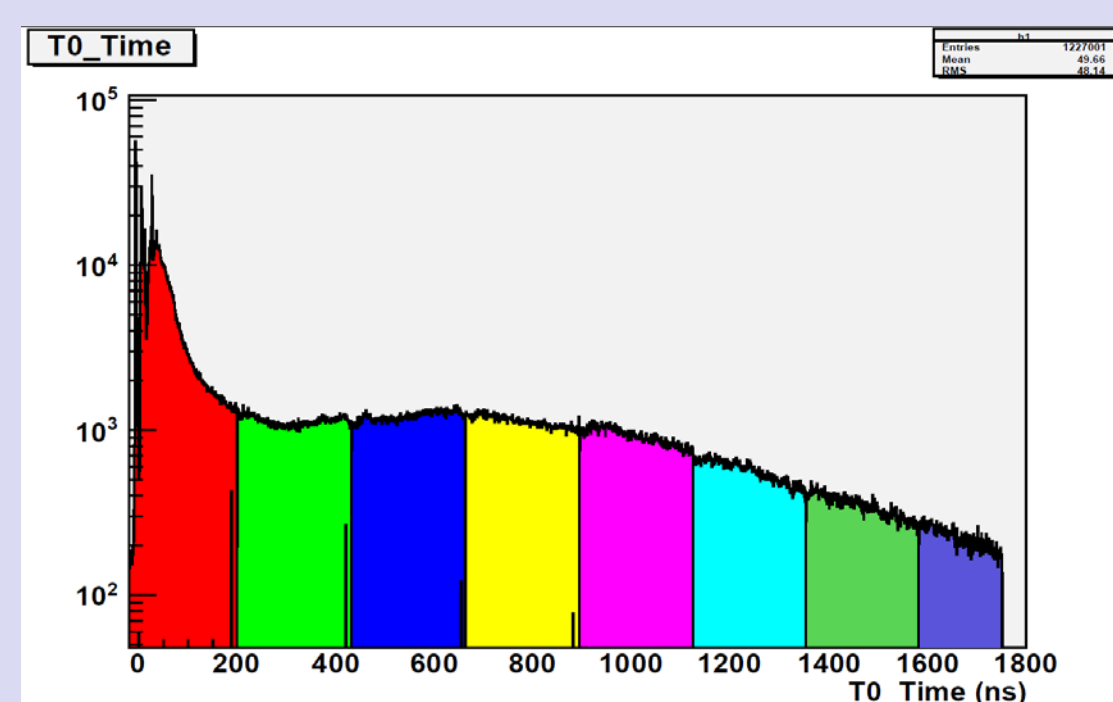


Cross sectional measurements of  $H(n,d\gamma)$  from 1 keV to 10 MeV. [3]

Precise measurements of this cross section have not been made, especially in the energy range relevant to Big Bang Nucleosynthesis. At left, the world’s data set for this reaction is sparse at best, with very little data at all in the range from 100 keV to 1 MeV. For this reason, this experiment attempts to measure this cross section for incident neutrons with kinetic energies from 100 keV to 1 MeV. The Clinton P. Anderson accelerator allows us to get a smooth distribution of all of these incident neutron energies at once, making the Los Alamos National Laboratory the ideal facility for this experiment.

## IV. Electronics Circuit

The electronics for this experiment are set up to record the pulses from the detectors. The most important part of the electronic setup is the trigger system. Depending on how many detectors and which detectors record a pulse, a trigger is created to record data on all the detectors. These triggers include singles events for the active target (a coincidence of top and bottom), BrillLanCe, and neutron detectors. It also includes coincidences between the active target and each of the other detectors—BrillLanCe, Neutron Detector 1, and Neutron Detector 2. For the neutron capture experiment, the coincidence of the active target and BrillLanCe is used to determine deuteron formation events.

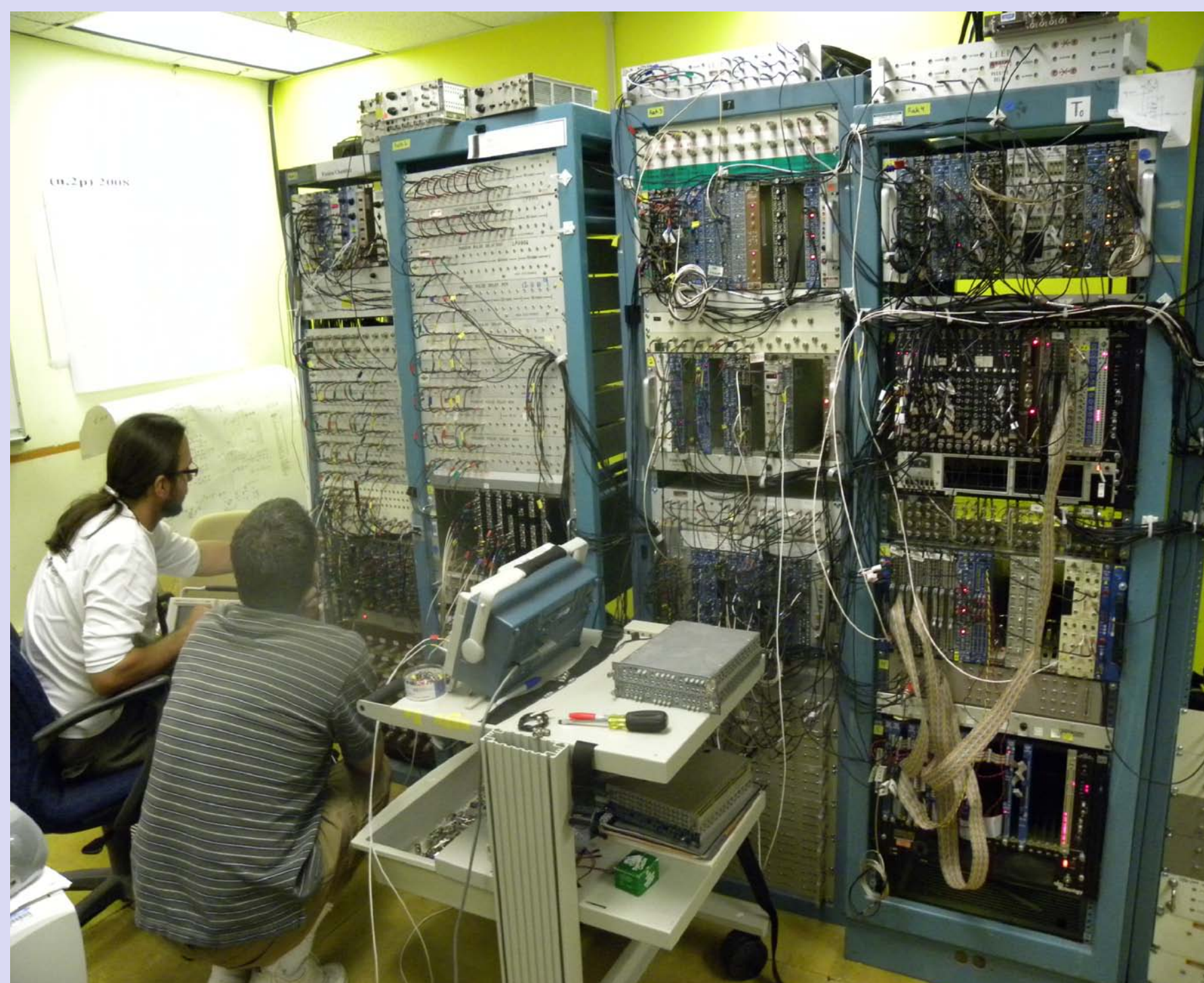


The  $T_0$  spectrum with each of the  $T_0$  copies pasted together to form the entire spectrum (Left).

To ensure the pulse read in by the electronics is the one that triggered the system, narrow digital gates are created around the pulse. In this way, misidentification of the triggering pulse is significantly reduced.

The result of the electronic system is that analysis can then proceed smoothly with a good guarantee that the data collected are the appropriate data.

An innovative part of the electronic system involves a floating gate. Since the experiment is interested in low energy incident neutrons, it is important to have high time resolution at the lower energies. To do this, the  $T_0$  pulse is copied 16 times, with each copy delayed by a different amount. The various copies of  $T_0$  can then be pasted together and used to create an energy spectrum with a 250 ps resolution.



FERA modules read the electrical outputs of the circuit into the computer for analysis.

## III. Experimental Apparatus

### A. Fission Chamber

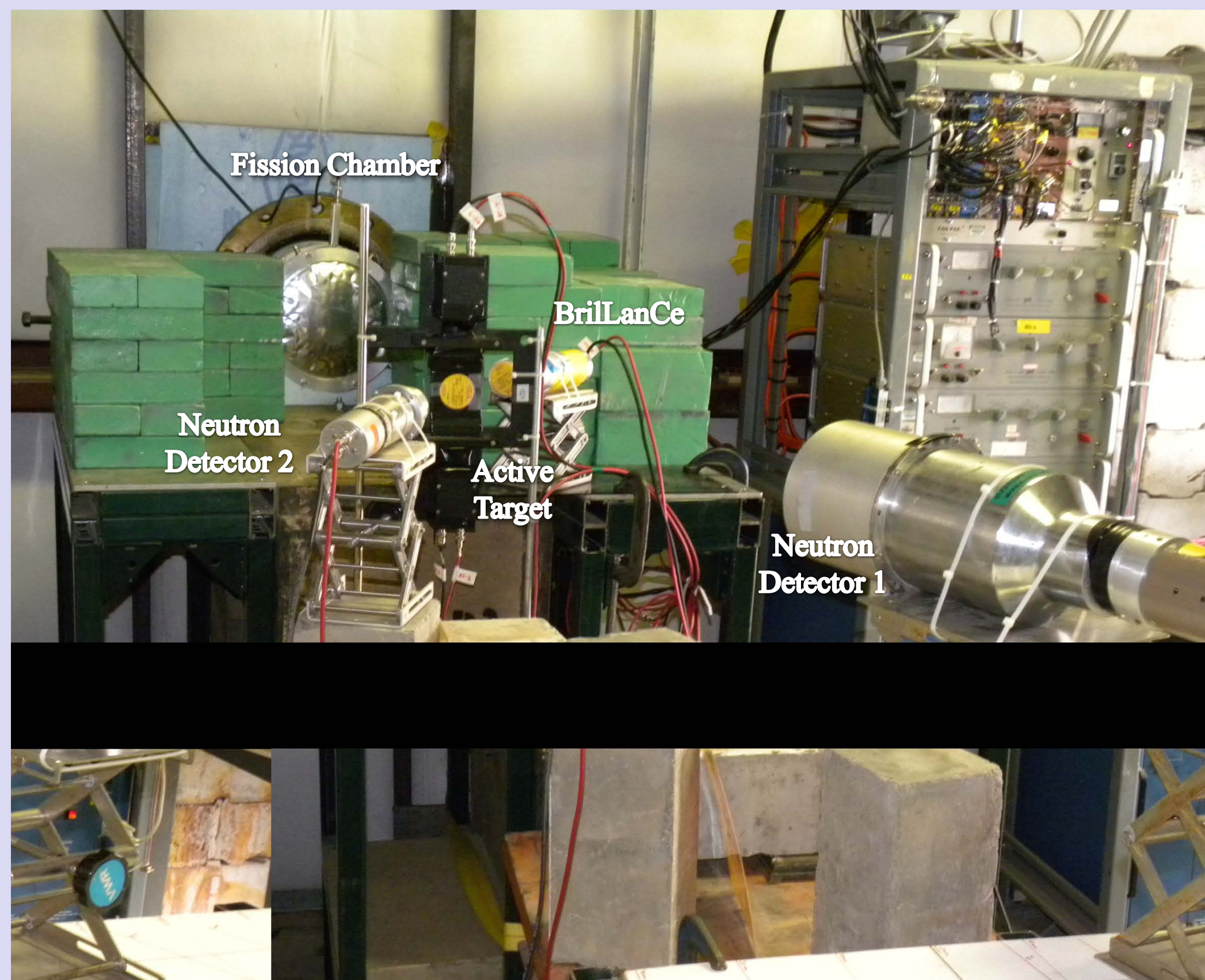
The incident neutron flux must be monitored to obtain an absolute cross sectional measurement. This is accomplished using a fission chamber, which is a cylindrical chamber filled with a 90% argon and 10% methane gas mixture. The chamber contains eight steel foils, one of which has a  $U^{238}$  deposit electroplated to it. The incident neutron beam induces fission in the uranium, and the fission fragments ionize the gas. Since the blank steel foils are held at a 300 V difference to the foil with the deposit, the charge from the ionized gas is attracted to the collecting foil, which then reads out pulses to an ADC and TDC for each alpha particle and fission fragment. The ADC pulse height is used to distinguish alpha particles from fission fragments, so the number of fission events can be determined. The TDC pulses are used to determine the energy of the incident neutron using time of flight.

### B. Active Target

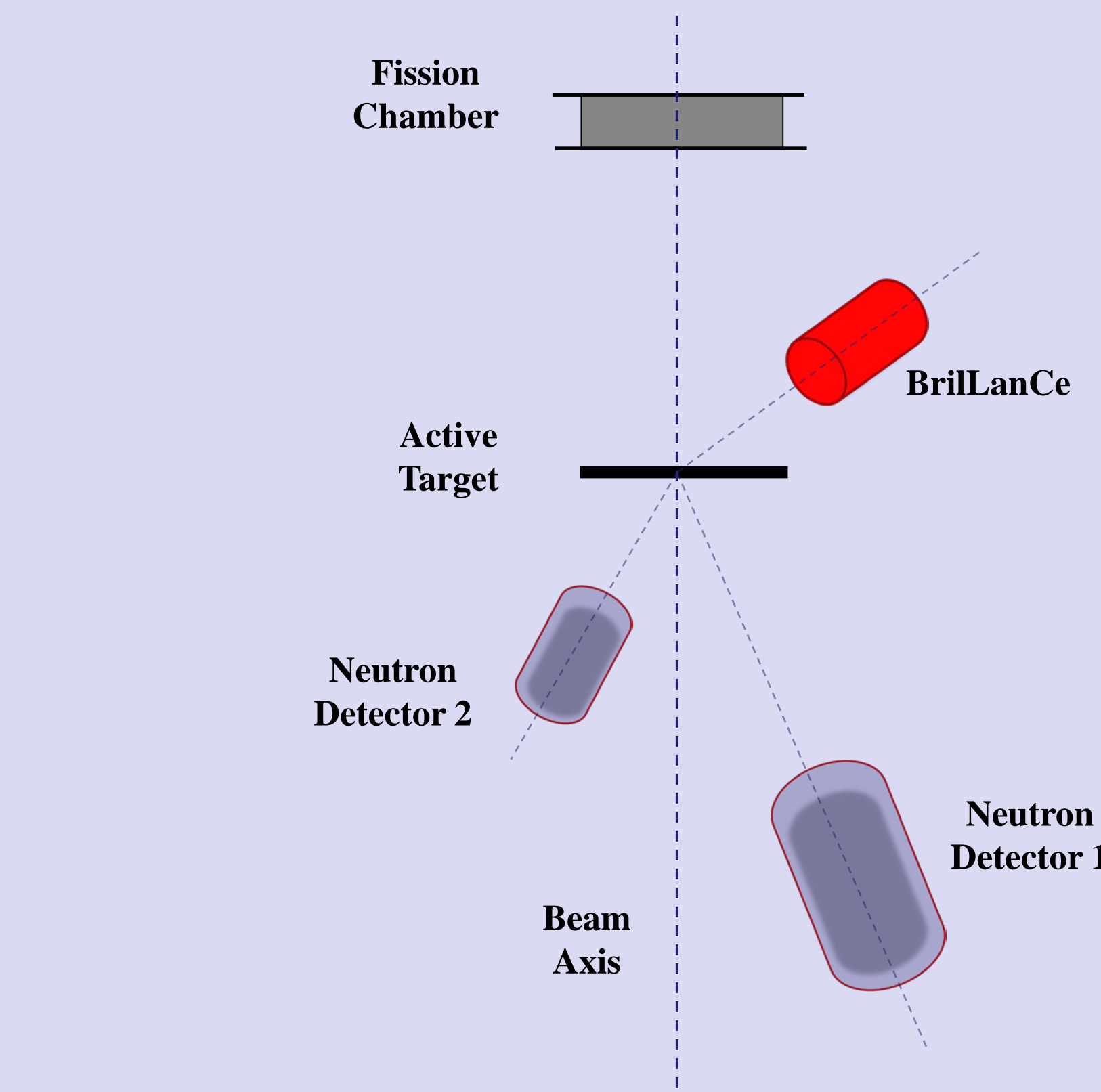
After the neutron beam from Target 4 passes through the fission chamber, it strikes the target. The active target is a 2mm thick BC-418 plastic scintillator with two photomultiplier tubes attached to it.

The active target is able to detect charged particles recoiling from neutron interaction because the ionizing radiation causes scintillation—a flash of light—in certain organic materials. When the ionizing radiation passes through the material of the detector, it excites the atoms to a higher energy state. Some of the energy is lost through lattice vibrations in the form of heat, resulting in a lower excited energy. The atoms de-excite to ground state by emitting a photon, which can then be detected by the photomultiplier tubes attached to the detector.

Events are only accepted if both the top and bottom photomultiplier tubes receive a signal. This scintillator is used to detect recoil deuterons from neutron capture and protons from neutron scattering.



The experimental setup from downstream of the neutron beam.



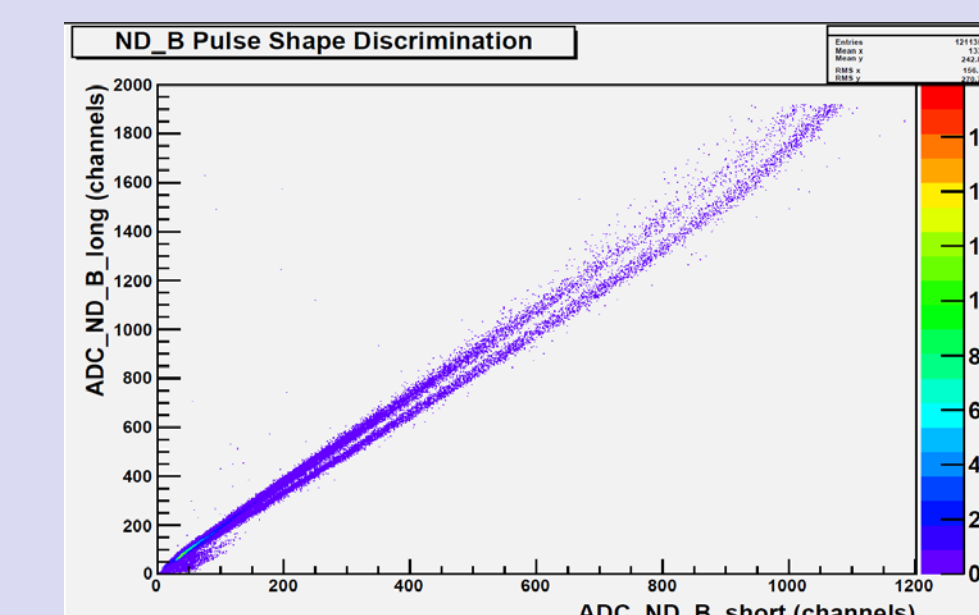
Schematic of the detector setup. The incident neutron beam (from top) is incident on the fission chamber and the active target. Gamma rays from deuteron formation are detected in BrillLanCe and the neutron detectors are used to calibrate the active target.

### C. BrillLanCe

To detect gamma rays released in neutron-proton capture, we use a BrillLanCe 380 detector made of  $LaBr_3(5\%Ce)$ . The advantages of this detector include high light yield, fast emission, and superior energy resolution at room temperature. This allows us to measure the energy of the emitted gamma rays, expected to be 2.225 MeV plus half the incident neutron kinetic energy.

### D. Neutron Detectors

Most neutrons interact with the protons by scattering off them, rather than forming deuterons. These neutrons are scattered elastically, so by detecting neutrons in liquid scintillators located at particular angles in coincidence with recoil protons in the active target, the cross section of elastic scattering can be used to determine the energy of the recoil proton and thus calibrate the active target.



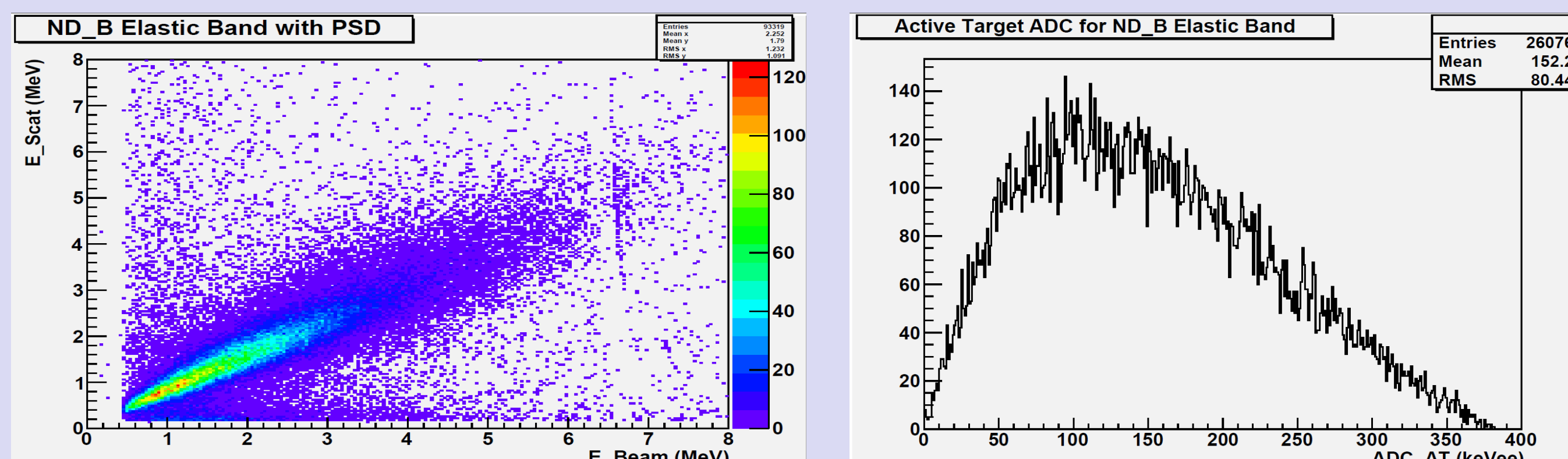
Histogram used to discriminate between neutrons and gamma rays detected in the neutron detectors.

Pulse shape discrimination is used to differentiate whether the pulses from the neutron detectors come from neutrons or gamma rays. To do this, the pulse is gated by a short and a long gate. The short gate is used to integrate only about half the pulse, whereas the long gate includes the pulse’s tail. In the histogram at right, the neutrons form the top band, whereas the lower band is made of gammas. Cuts can be made on this plot to choose only the neutron events for np elastic scattering.

## V. Analysis

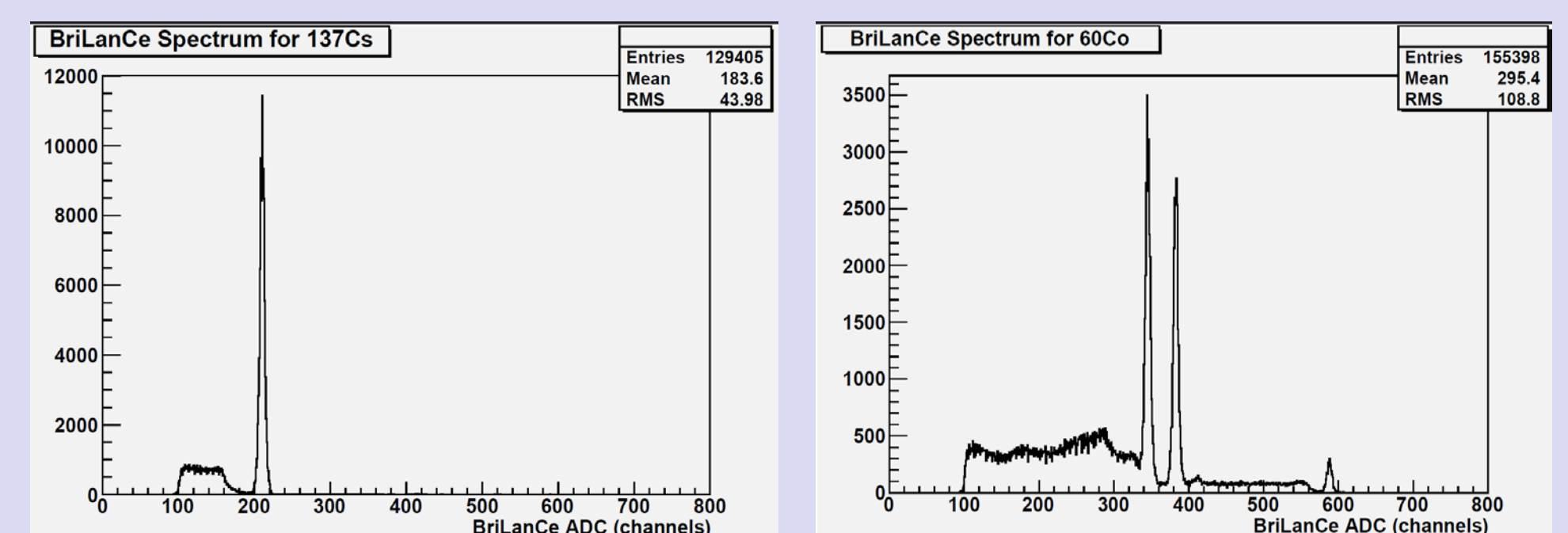
To find the differential cross section for  $n + p \rightarrow d + \gamma$ , it is necessary to determine the energies of the incident neutron, scattered deuteron and gamma ray. The incident neutron can be found using time of flight (TOF). The flight path distance from Target 4 is known and a  $T_0$  pulse is sent to the electronics every time a proton pulse impinges on the tungsten target, so the start time is also known. The TDC spectrum of the active target can then be used to find the time a neutron interacted with a proton in the active target, indicating its arrival time. From the times and distance, the velocity and hence energy of the incident neutron can be determined.

From the geometry and knowledge of the energy of the incident neutron, the energy of the scattered neutron and recoil proton can be determined. This can be used to calibrate the active target ADC spectrum by comparing the recoil proton energy with the associated ADC pulse height.



On the left is a 2-D histogram of scattered neutron energy vs incident energy. Note the clear elastic band along the diagonal. The right histogram is the ADC spectrum of the active target cut on the elastic band seen at left.

Radioactive sources like Americium-141, Cesium-137, and Cobalt-60 are used to calibrate the detectors as seen below.



On the left is a histogram of the ADC spectrum of BrillLanCe with a Cs-137 source and the right is a histogram of the ADC spectrum of BrillLanCe with a Co-60 source.

## VI. Conclusion

Analysis of the data collected is still underway, although significant progress has been made. It will continue to be analyzed to find differential cross sections for the  $H(n,d\gamma)$  reaction.

### Bibliography

[1] D.N. Schramm and M.S. Turner, Rev. Mod. Phys., 70, 303 (1998)

[2] Y. Nagai et al., Phys. Rev. C, 56, 3173 (1997).

[3] A.Tomyo et al., Nucl. Phys. A718, 401c (2003).